

RESEARCH ARTICLE

Connect-while-in-range: Modelling the impact of spatial constraints on dynamic network structures

Niek Kerssies^{1,2*}, Jose Segovia-Martin^{1,3}, James Winters⁴

1 School of Collective Intelligence, University Mohammed VI Polytechnic, Rabat, Morocco, **2** Department of Sociology, Rijksuniversiteit Groningen, Groningen, The Netherlands, **3** Complex Systems Institute of Paris Ile-de-France, Centre national de la recherche scientifique, Paris, France, **4** Centre for Culture and Evolution, Department of Psychology, College of Health, Medicine and Life Sciences, Brunel University London, London, United Kingdom

* niek.kerssies@um6p.ma

Abstract

Like other social animals and biological systems, human groups constantly exchange information. Network models provide a way of quantifying this process by representing the pathways of information propagation between individuals. Existing approaches to studying these networks largely hypothesize network formation to be a result of cognitive biases and choices about who to connect to. Observational data suggests, however, that physical proximity plays a major role in shaping the formation of communication networks in human groups. Here we report results from a series of agent-based simulations in which agents move around at random in a bounded 2D space and connect while within range. Comparing the results to a non-spatial model, we show how including spatial constraints impacts our predictions of network structure: range model networks are more clustered, with slightly higher degree, higher average shortest path length, a lower number of connected components and a higher small-world index. We find two important drivers of network structure in range model networks: communication range relative to environment size, and population density. These results show that neglecting spatial constraints in models of network formation makes a difference for predicted network structures. Our simulation model quantifies this part of the process of network formation, realized by simply situating individuals in an environment. The model also provides a tool to include spatial constraints in other models of human network generation, as well as dynamic models of network formation more generally.

OPEN ACCESS

Citation: Kerssies N, Segovia-Martin J, Winters J (2025) Connect-while-in-range: Modelling the impact of spatial constraints on dynamic network structures. *PLoS Complex Syst* 2(7): e0000051.
<https://doi.org/10.1371/journal.pcsy.0000051>

Editor: Qinghua Chen, Beijing Normal University, CHINA

Received: October 16, 2024

Accepted: May 12, 2025

Published: July 1, 2025

Peer Review History: PLOS recognizes the benefits of transparency in the peer review process; therefore, we enable the publication of all of the content of peer review and author responses alongside final, published articles. The editorial history of this article is available here: <https://doi.org/10.1371/journal.pcsy.0000051>

Copyright: © 2025 Kerssies et al. This is an open access article distributed under the terms of the [Creative Commons Attribution License](https://creativecommons.org/licenses/by/4.0/), which permits unrestricted use, distribution, and reproduction in any medium, provided the original author and source are credited.

Data availability statement: This model was coded in Python using the Networkx package. The code including detailed instructions is publicly available on github: <https://github.com/niekerkssies/Range-model>.

Author summary

Much like neuroscientists require a solid understanding of the connections between each neuron in order to understand cognition, we need a solid understanding of communication pathways between individuals in order to understand the collective intelligence of groups. One major difference from brains is that individuals can move around in an

Funding: The author(s) received no specific funding for this work.

Competing interests: The authors have declared that no competing interests exist.

environment, constantly changing communication networks. We simulated this dynamic effect of movement in an environment on network structure, by simulating a population of agents moving around in a 2D coordinate space and forming temporary connections while within a specified range. These simulations allowed us to understand the formation of networks under different spatial circumstances, quantifying the impact of communication range, population size and environment size on the properties of the resulting networks. This allows us to understand part of human networks without assuming individual connection preferences, focusing instead on the basic fact that people exist and communicate in an environment.

1. Introduction

Like other group-living animals and like other biological systems such as brains, human populations form collections of individual components that exchange information. Network models can mathematically represent the pathways along which this information is transmitted between individuals. Networks (sometimes called graphs) are mathematical representations of relationships (links or edges) between individual objects (nodes or vertices). The way in which nodes are connected is called network structure. Differences in network structure and properties in human groups have been shown to correlate with differences in outcomes of collective processes such as information diffusion, collective intelligence, and cultural evolution [1–7] (although not the main focus of the current paper, we discuss some examples of these results below; for excellent reviews, see [8,9]).

Where this body of research investigates mostly static network structures selected by researchers, other work has studied the shape and drivers of networks in real human groups. One category of hypotheses suggests network structure to be a result of rules of individual cognition: following preferences, biases, or strategies, individuals select others to connect to. Social science research, for example, has identified many consistent patterns in human social networks, including the tendency for people to have social ties with others that have characteristics in common with them (homophily), and of well-connected individuals to accrue disproportionately more connections over time [10,11]. Experiments that allow for participants to change network ties have found a tendency to connect to the highest-scoring participant in a task setting [12–14]. Fieldwork and experiments in cultural evolution have studied “model-based biases” by which human and nonhuman animals select others to socially learn from, such as the preference to copy from higher-ranked individuals found in some primates [15–19]. Our intention here is not to give an exhaustive overview of such forces. Rather, it is to contrast these contributions to network structure of individual preferences, to the contribution of other types of forces. In order for individual preferences to fully explain network structure, each individual needs to be able to choose from the complete population; yet there are social [20–26] as well as physical reasons [27–29] why the pool of individuals to choose from is ‘pre-selected’ by circumstances. In this paper, we are interested in isolating the effect of these physical reasons: because individuals exist and move in an environment, and because communication takes place on physical media that have limited effective ranges, physical constraints pre-select the network structures that are possible.

Observational data suggests an important role for physical proximity in the shape of human social and communication networks [27–29]. Even in data from online social media and mobile communication, where distance would seem intuitively to be less of a constraint, networks are shaped significantly by geography and existing real-world social ties [30–33]. In this paper, results are reported from a series of agent-based simulations designed to study

the question: how does including physical proximity and limited communication range in a model impact our predictions of network structure? In our model, agents randomly move through a bounded 2D coordinate space and connect to others only while within a specified range. The resulting network structures represent the physically possible interactions that agents can choose from, set by physical constraints. These networks are compared to results from a non-spatial model, without positions and movement, in which agents connect and disconnect at random. Like a recent model by Chimento and Farine [34], the model simulates the impact of movement through a 2D space on network structure and information transmission. In their paper, statistics of dynamic networks are compared to properties of cumulative interaction graphs (static networks composed of interactions combined over time), showing differences in network structure predictions. Our results include dynamic graph statistics only. Unlike their model, in which population size and range stay constant, we consider the complete meaningful parameter space of communication range and population density, mapping the influence of these parameters on 6 network structure measures, from N disconnected components to fully connected networks. Our model is also like a cellular automata model by Vining and colleagues [35] where agents move randomly through a 2D space and connect within range, though they focus on the impact of spatial constraints on performance on a consensus task, rather than network structure outputs.

We find that introducing location, random movement and ranged communication introduces much more clustered networks, with slightly higher degree, higher average shortest path length, a lower number of connected components and a higher small-world index than a dynamic non-spatial model. All of these differences are more extreme when range is low. Our model shows how simply locating individuals in an environment changes our predictions of the network structures that can form, and provides a tool for including spatial constraints in models of network formation. The consequences of these network structure differences are highlighted by several types of information transmission which we include in the simulations, replicating known effects of network structure on these processes.

2. Materials and methods

2.1. Model

2.1.1. Random movement and the range rule. In agent-based models, each of a population of agents follows an update rule every timestep. In this model, the model parameters are N , g and r . N is the population size, g is the grid size such that $g \times g$ is the area of the coordinate space, and r is agent communication range. N agents are initialized and assigned a unique random coordinate value (x, y) within the $g \times g$ grid.

Each timestep, every agent (1) moves, (2) connects, and (3) disconnects. To move, an agent chooses from a uniformly random distribution of its adjacent integer coordinates, including its current location. To keep agents within the bounded space and to prevent agents sharing the same position, adjacent coordinates with values below 0 or exceeding g , or currently occupied by other agents, are excluded from the random selection of a new position. If all adjacent coordinates are out-of-bounds or occupied, the agent remains in the current position.

To connect, after moving, each agent creates an undirected network link with all other agents that are currently in range. Range is calculated as Euclidean distance in the coordinate space, rounded to integer values for x and y . Euclidean distance uses the Pythagorean theorem that for right-angled triangles, $c^2 = a^2 + b^2$ (where a and b are the base and altitude, and c the hypotenuse of the triangle). Agent i checks whether agent j is in range by putting the difference in coordinates $x_j - x_i$ and $y_j - y_i$ as a and b , and calculating the distance to j as c ; so $r = \sqrt{(x_j - x_i)^2 + (y_j - y_i)^2}$. If the result is less than or equal to the value of r , agent j is

within range. Finally, to disconnect, the agent deletes any links with agents that are no longer in range. The order in which agents are updated is randomized each timestep. Fig 1 shows the initialization and first timestep of a possible model run schematically.

A note on model ontology. For purposes of clear understanding, our model is intentionally very simple, varying only three parameters. One consequence is that the model is very generally applicable. Agents can be any group of moving components that make any type of proximity-constrained connection. One possible interpretation this leaves open is the 2D grid as an abstract problem space, in which agents explore adjacent solutions (such as in [36–38]). Similarly, the space could be seen as an attribute or trait space, in which agents are “proximate” when they have similar attributes (akin to [39]). Though these are possible uses, the intended application is to represent the network of possible interaction partners available for individuals to choose from, as constrained by their embeddedness in a spatial environment, their ability to move in that environment, and the physical properties of communication. Nonhuman animals employ various communication media such as chemical, visual, tactile, and seismic signals, while humans additionally use technologies ranging from conversations to the Internet [30,40,41]. Each of these media has an effective range, that interacts with movement and position in an environment to constrain the possible networks of interactions between individuals. Though the intended application is human networks, this general interpretability is part of the point: we aim to model properties that human groups have in so far as they are also physical communication systems. We hope that as a consequence, our findings are also useful for nonhuman applications such as inferring interaction networks from animal movement and location data, and programming communication networks in swarm robotics based on relative positions alone [42,43].

2.1.2. Null model. The intention of the simulations reported in this paper is to demonstrate the work being done by spatial constraints in network formation. In order to do so, the results are compared to a non-spatial model. In the non-spatial model, each timestep agents simply connect to each other agent with probability $P(\text{connect})$ which is set globally as the same for all agents. In order to compare this model’s outputs to that of the range model, N can be set to the same value or varied in the same range of values, while $P(\text{connect})$ corresponds

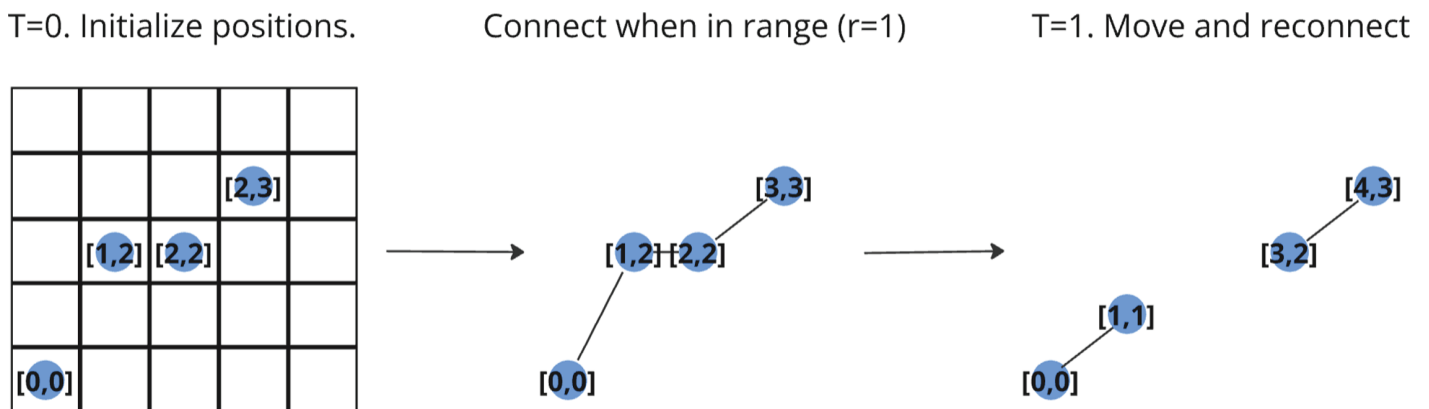


Fig 1. Demonstration of a possible initialization and timestep in the model for $N = 4$, $r = 1$, $g = 4$. Agents are randomly assigned a unique (x,y) coordinate. The coordinate space is graphically represented here as a grid(left), and agents are shown with their coordinate values. At every timestep, every agent follows the range rule: if the Euclidean distance between the agents is less than or equal to r , a link is created between them. Thus, from the initial position shown on the grid, the graph shown in the middle of the figure is formed. At the start of the next timestep, agents move at random and follow the range rule again. When previously in range agents are now out of range, the link is cut. Hence, from every agent performing random movement and following the range rule, a new network is formed.

<https://doi.org/10.1371/journal.pcsy.0000051.g001>

to r . Like r , the $P(\text{connect})$ parameter can be varied through its whole meaningful range of values, from isolated agents to fully connected networks. A connection probability of 0 will mean N unconnected agents, while a probability of 1 will always create fully connected networks. The parameter g has no equivalent in the non-spatial model and there are no coordinates assigned to agents. Finally, in order to make the non-spatial model a dynamic process as well, a random disconnect chance is included, which is set to $1 - P(\text{connect})$. This way, the probabilities of connecting and disconnecting mirror those of the range model, as the area not covered by an agent's range is equal to the inverse of the area covered (for a calculation of connection probability under random movement and ranged communication in an unbounded space, see [35]).

2.2. Sensitivity analysis setup

Simulations consisted of several sensitivity analyses. In each such analysis, one of the model's three input parameters N, g, r was chosen to vary while the others remained constant. For each integer value of the varying input parameter, both the range and the null model ran for 100 rounds of 100 timesteps, where at each timestep, all agents were updated in a random order and output measures were collected.

For the first set of analyses, range was varied between $r = 0$ and $r = 10$ while N was kept at constant values, varying between tests from $N = 1$ to $N = 100$ (see Fig 2 for results for $N = 20$; see S2 Appendix, S2 Fig and S3 Fig for, 40, 60, and 80). Varying range up to $r = g$ ensures that in terms of network structure, the complete meaningful range of r -values is tested. At $r = 0$, no agents are connected; at $r \geq g$, where the diameter of each agent's range covers the whole length of the coordinate grid, networks are always fully connected. In the null model, the connection probability parameter $P(\text{connect})$ was varied between 0 and 1 with intervals of 0.1, similarly ensuring that the simulations start at disconnected agents and end at fully connected networks.

In the second set of analyses, in each test N in both the range and the null model was varied between 1 and 49, while $g = 7$ and r varied at constant values between tests, from 0 to 7. N varies up to 49 because when $g = 7$ there are $7 \times 7 = 49$ unique positions in the environment. Since agents avoid sharing the same position, as N increases towards $g \times g$, the space becomes increasingly "crowded" until it is completely saturated and agents remain in place, each in a unique position. For this parameter, then, the meaningful range is determined by population density $N/(g \times g)$, varying between $1/49$ at $N = 1$ and $49/49 = 1$ at $N = 49$. Since it lacks spatial positions, the null model (or any other nonspatial model) has no analog to g . We therefore show results here only for varying N ; for varying g , see the S3 Appendix and S4 Fig. In the null model, N was varied over the same values while $P(\text{connect})$ was set to r/g . This way the null model mimics the connection probability of the range model, in which an agent's probability to connect is proportional to the range relative to the environment size. Table 1 summarizes the model parameters and the ranges in which they were tested.

2.3. Output measures

Each timestep, 6 network properties were calculated in both models. The network properties calculated are average degree, clustering coefficient, average shortest path length, number of connected components, size of largest component, and small-world index. Here, we briefly explain how these metrics are calculated, motivate why we include them, and what they can show about the properties of a network. We chose measures that give a clear general overview of network structure. Since the model attempts to capture pathways for information transmission, we focus on macro-level properties that are known to have relevant impacts

Table 1. Overview of model parameters and ranges tested.

Model	Parameter	Symbol	Explanation	Values Tested	Constant parameter values
Range	Communication range	r	When the Euclidean distance between agents i and $j \leq r$, create link ij .	(0,10)	$N = 10, g = 10$
Range	Population size	N	Number of agents.	(1,49),60,80,100	$r = 2, g = 7$ (for 1,49), $g = 10$ (for 60, 80 and 100)
Range	Grid size	g	Defines the coordinate space $g \times g$.	(1,50)	$r = 2, N = 10$
Null	Connection probability	$P(\text{connect})$	Probability of connecting to each other agent each timestep.	(0,1) (increments of 0.1)	$N = (1,49),60, 80,100$
Null	Disconnect probability	$P(\text{disconnect})$	Probability of cutting an existing connection each timestep, always $1 - P(\text{connect})$.	(0,1) (increments of 0.1)	$N = (1,49),60, 80,100$

<https://doi.org/10.1371/journal.pcsy.0000051.t001>

on the diffusion of information. To an extent, the choice for these measures is arbitrary, and future research stands to benefit from studying the effects of our model parameters on more individual and meso-level measures such as degree distributions and community formation.

Networks are mathematical representations of relationships (edges or links) between objects (nodes or vertices). Degree is a property of single nodes: the amount of connections a node has in the network. The average degree K is simply the population average of node degrees k_i : $K = \frac{\sum_{i=1}^N k_i}{N}$. In this model, agents are network nodes. Agents do not connect to themselves, and redundant connections are not possible. Therefore, the maximum amount of connections one agent can have is $N-1$. For a population of 10 agents, average degree will therefore be a value between 0 and 9. Note that if the population average degree is equal to $N-1$, this indicates a complete graph: the network where each agent is connected to all other agents. This measure, then, gives a simple and intuitive indication of where the network is on the spectrum between completely disconnected and fully connected, while retaining information about the number of connections of each agent.

Clustering indicates the fraction of a node’s network neighbors that are themselves connected to each other. To illustrate, say agent A is connected to three others B, C and D. B and C are connected, but C and D are not and neither are B and D. In this case, ABC forms a fully connected triangle, while ABD and ACD do not. Clustering can be indicated as the ratio of actual to possible fully connected triangles, in this case $1/3$. This is the clustering coefficient. This coefficient is calculated for the whole network each timestep, resulting each time in a value between 0 and 1. Note that a value of 1 for this coefficient corresponds to the complete graph at which average degree is $N-1$; if all possible triangles are fully connected, then the whole network is fully connected. Clustering is an indicator of how “local” and redundant a network’s connections are. The opposite of a very clustered network we might call a fully ‘hierarchical’ or ‘efficient’ network, where all nodes connect back to a single node or small group of nodes [44]. A signal across such a network spreads very efficiently, taking 1 step to reach the ‘leader’ node(s) and 1 step back to reach all others. In contrast, a signal across a very clustered network can take many steps to travel between any 2 given nodes if it lacks long ties between local ‘neighborhoods,’ and the traveling signal can become “stuck” in local clusters. More clustered networks have therefore been shown to slow down processes of diffusion

across populations, but also to increase performance in the exploration of more complex task spaces, by slowing down conformity to a single central solution [4–6].

The shortest path length between two nodes is the minimum amount of links that need to be traversed in order to get from one to the other. Average shortest path length is the average taken over all node pairs. Here, too, an average value of 1 means that the networks are fully connected, since it indicates that all agent pairs have a direct path of 1 link between them. In terms of diffusion across the network, average shortest path length has a comparable but inverse effect to clustering: spreading processes will be slower when shortest path lengths are high. In fact, this measure is a direct indicator of the time any type of diffusion will take to spread across a network. Note that since networks in this model often form several disconnected components, the average shortest path length is often calculated separately for each component, and then averaged.

In this model, the agents will not always form a single network. More often, especially at low range (and at low connection probability in the null model), the population will consist of several mutually unconnected local networks, or single isolated agents. To keep track of this, we calculated the number of such connected components and the size of the largest connected component. When the number of components is 1, the population forms a single connected graph; when it is equal to N , no agents are connected. Conversely, when the largest component is equal to N , the population forms a single connected graph, and when it is 1, no agents are connected. This measure is useful to include if we're interested in diffusion processes on the network: whatever the structure indicated by the previous three measures, as long as networks do not form a single component, nothing that starts in single agents will spread across the whole network. Note that a population that forms a single connected network, where there is at least one path between all agents, is not necessarily a fully connected network, where there is a direct link between all agents.

Finally, we calculated the small-world-index of networks. Strictly speaking, a small world network is one defined by the parameters n, k and p , where n is the population size, k is the number of neighbors on a ring lattice that each node connects to (therefore each node has the same degree k). Parameter p is the probability that a link is “rewired”: replaced by a link to a node chosen at random from the whole population [44]. A direct comparison between a small-world networks and range model networks, however, does not make much sense, for two reasons. First, the range model is a spatial model: in a small-world network, nodes have a fixed position on a ring lattice, while in the range model, agents move around through a 2D coordinate space. Second, in a small-world network k specifies a global degree value. When rewiring probability p is 0, this means that all nodes have degree k . This is very rare in a dynamic, spatially explicit model with random movement; it can only occur when agents happen to form an equidistant ring in space.

In order to still have an indication of the occurrence frequency of small-world-like structures, there is the small-world index [45]. The small-world index S of a graph G is the ratio of C to L . C is equal to CG/CR , where CG is the clustering coefficient of G , and CR is the clustering coefficient of a random graph with the same number of n nodes and m edges as G . Similarly, L is equal to LG/LR , where L is the average shortest path length. S , then, is calculated as $S = (CG/CR)/(LG/LR)$. This measure captures the feature of small-world graphs that most nodes are locally connected, while some are rewired to form ‘longer’ ties outside of local clusters. Adding only a few of such long ties connects relatively clustered local communities, creating much shorter average shortest path lengths while keeping clustering high [44]. If, therefore, clustering is low and average shortest path length is high compared to a random model, S will be low; if the opposite is the case, S is high. Small-world networks were designed specifically to generate properties specific to human networks, which exhibit high clustering and low

average shortest path length [44]. They have also been studied in terms of impact on information diffusion [2,9]. Having an indication of small-world-ness in our output measures helps pinpoint the circumstances under which there could be spatial contributions to the generation of these well-studied network structures. Note that at low range and low population density, both the null and the range model can often generate a population of completely isolated agents: an empty graph. In such a situation, both the clustering coefficient and the average shortest path length can be 0 in some runs. Since small-world index uses these measures in the denominators of fractions, such cases would require division by zero, leading the index to be undefined. We chose to simply exclude these runs, leading to the apparent lack of data at $r = 1$ in the lower right panel of Fig 2, and at lower values of N (see below).

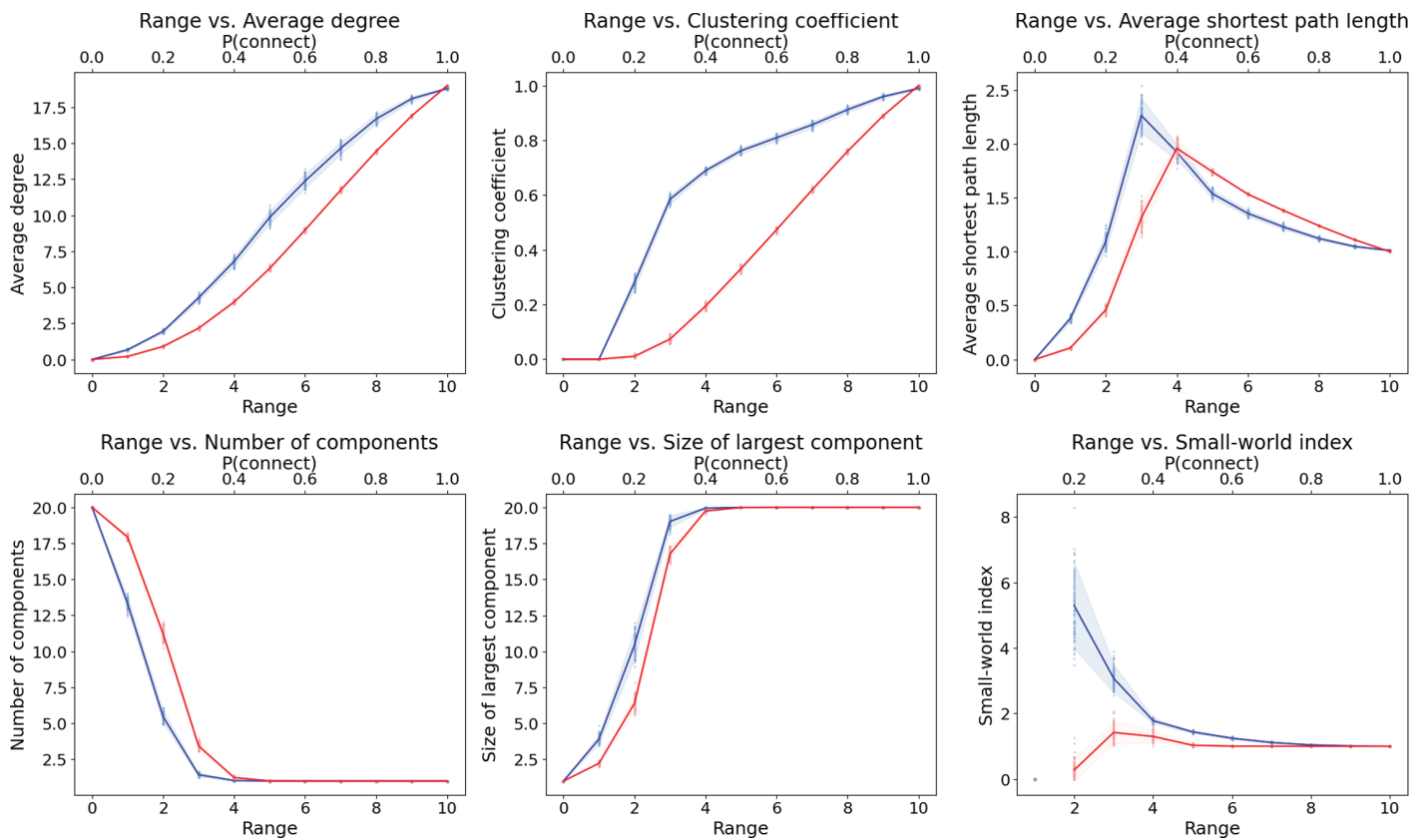


Fig 2. Network properties of range model and null model networks for varying range, $N = 20$, $g = 10$. Range model results are shown in blue; null model results in red. Range was tested for each integer value from 0 to 10, shown on the bottom labels of the x-axis. The null model $P(connect)$ parameter was tested at r/g for each of these values, shown on the top labels of the x-axis. At each of these values, both the range and the null model were simulated for 100 rounds, each of 100 timesteps. Each network measure was collected at each timestep, and the dots shown in the figures represent time-averaged network measures for each round. Lines are drawn through the means of these time averages purely as visual aid, while transparent areas show 1.5 standard deviations. At low range settings (when spatial constraints are most articulated), networks are much more clustered, have slightly higher degree, higher average shortest path length, a lower number of connected components and a higher small-world index than the null model (for $N = 40, 60, 80$ and 100 , see S2 Appendix, S2 Fig, and S3 Fig).

<https://doi.org/10.1371/journal.pcsy.0000051.g002>

3. Results

3.1. Spatial constraints create networks with higher clustering and lower average shortest path length

The most conspicuous difference between the range model and the null model is the difference in clustering. As can be seen in the upper middle panel of Fig 2, clustering is much higher in the range model at all settings except fully connected networks. This difference is particularly visible at lower values of r . Part of this difference in clustering is accounted for by the difference in average degree. As range and connection probability increase, agents form more connections, leading to higher population average degree. As more of the possible connections between agents are made, more connected triangles form, increasing the clustering coefficient. In the non-spatial null model, this effect seems to account for the increase in clustering, which closely follows the increase in degree (Fig 2 top-left and upper middle panels). In the range model, however, this straightforward relationship between degree and clustering is not observed, especially at lower values of r . This is because there is an additional effect increasing clustering, introduced by range-constrained network formation. Since movement is random, the probability of two agents A and B being within range and therefore connected is well-modelled as a random process. If we simplify B's random walk up until this timestep by assuming its current location is drawn uniformly at random from the coordinate space, its probability to connect to A is proportional to the percentage of the area covered by A's range: $P(AB) \propto 2\pi r/g^2$ (see for a formal treatment in unbounded space [35]). Given a connection between A and B, a third agent C follows the same probability of connecting to A. However, once both A and C are connected to B, we can limit our assumption of their possible current positions, from the entire coordinate space g^2 , to the area covered by A's range $2\pi r$, making it much more likely for B and C to connect as well and form an ABC triangle. Fig 3 illustrates

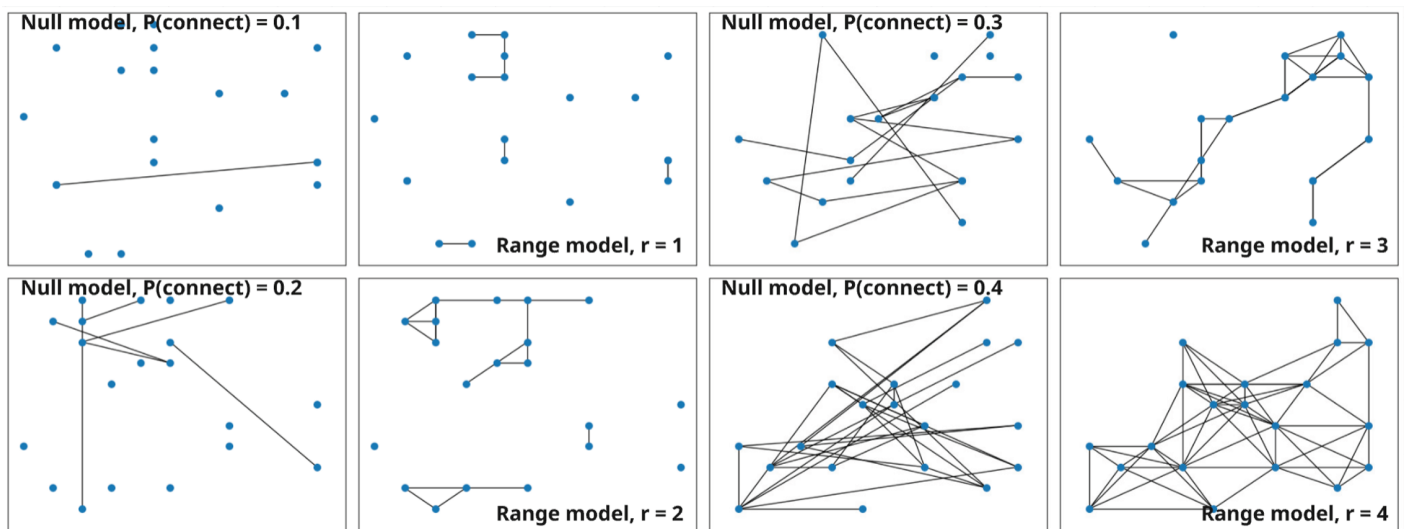


Fig 3. Four snapshots comparing null model to range model networks, $N = 18$, $g = 10$. Each snapshot is a timestep taken from a simulation round. In order to make visual comparison easier, the spatial layout created by the positions of the agents in the range model graphs are copied in the null model comparisons (which do not have positions themselves). At each timestep, the null model (left) is compared to the range model (right) at r/g . Upper left: $r = 1$, $P(\text{connect}) = 0.1$. Lower left: $r = 2$, $P(\text{connect}) = 0.2$. Upper right: $r = 3$, $P(\text{connect}) = 0.3$. Lower right: $r = 4$, $P(\text{connect}) = 0.4$. At similar connection probabilities, agents in the range model only connect to closer agents, creating more connected triangles.

<https://doi.org/10.1371/journal.pcsy.0000051.g003>

this difference with network visualizations, showing many more complete triangles in the range model compared to the null model at comparable settings.

This effect leads to networks with highly localized structure when $r:g$ is low, which is reflected in much higher clustering as well as higher average shortest path length. Low range “assorts” agents into local clusters of physical proximity. As r increases and the proximity constraint softens, these differences dissolve until resembling the null model. As a direct result of the large difference in clustering and average shortest path length, the range model networks have much higher small-world index when range is low. Introducing spatial constraints therefore produces more ‘small-world-like’ networks, most notably so when $r:g = 0.2$ (This values scales with N ; see S1 Fig). Although the non-spatial model often shows lower average shortest path length, the difference in clustering at low r is high enough for the range model to show a clear spike in small-world index (Fig 2, lower right panel). For discussion of results at other constant values of N , see S1 Appendix and S1 Fig.

3.2. Range constrains the influence of population density on network structure.

For constant values of r and g , varying population size N also impacts network structures in the range model. In both the null model and the range model, as population size increases, networks become more densely connected, and average degree increases. As has been shown for static Erdos-Renyi graphs, both models also show a critical value of N after which networks form a single connected ‘giant’ component [46]. The mechanisms, however, differ. In the null model, the increase in degree is a matter of increased possible links, which, with the same $P(\text{connect})$ but an increased number of trials, will lead to more links overall as well as per agent. In the range model, population size increases population density N/g^2 , which, much like increasing $r:g$, makes randomly moving agents increasingly likely to encounter other agents. Moreover, the range model exhibits an additional ‘crowding’ effect that leads to higher average degree as well as a higher rate of increase of average degree with N (as can be seen in the upper left panel of Fig 4). This crowding effect works as follows. In an unbounded space, it would be more accurate to assume an agent’s probability of randomly encountering and therefore connecting to another agent remains approximately constant. In such a model, N would only increase degree by increasing the number of times the model draws from this probability distribution, therefore increasing the number of successes, as is the case in the null model. In a bounded space, however, where agents cannot share positions, increasing population density means positions become less randomized by movement, and the area covered by any given agent’s range is more likely to contain more agents, until the coordinate space is fully ‘saturated’ and agents can no longer move. The result of this effect of population density is consistently higher degree than the null model, as well as a consistently lower ‘critical’ value of N at which the network forms a single component (see upper left and lower middle panel of Fig 4).

The fact that, as discussed above, the range model creates more locally structured graphs, is reflected in these results as well: the range model networks have consistently higher clustering and average shortest path length, and as a result, a higher small-world index (upper middle, upper right, and lower right panels of Fig 4). Range model networks do, however, show a much lower number of connected components (lower left panel of Fig 4): connections may be local, but high clustering as well as a bounded space mean that connections are redundant enough to be more likely than a random model to connect to larger portions of the population. Range model networks at low r form long, clustered chains of agents that form a large

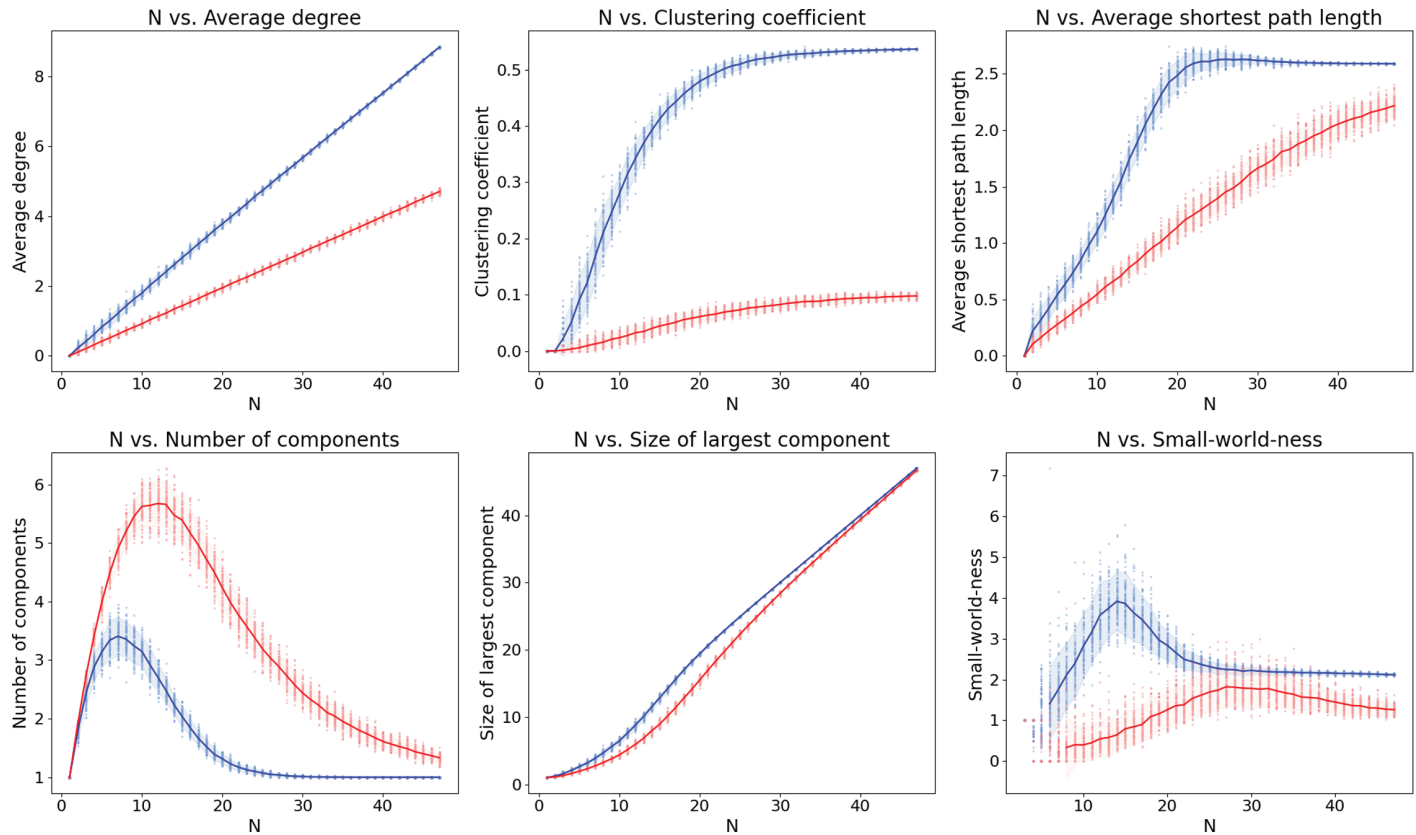


Fig 4. Network properties of range model and null model networks for varying population size, $r = 2$, $g = 7$. Range model results are shown in blue; null model results in red. In both models, population size was tested for all integer values between 1 and 49, shown on the x-axis. At each of these values, both the range and the null model were simulated for 100 rounds, each of 100 timesteps. Each network measure was collected at each timestep, and the dots shown in the figures represent time-averaged network measures each round. As visual aid, lines are drawn through the means of these time averages, while transparent areas show 1.5 standard deviations. Ranged networks show higher clustering, average degree, and average shortest path length, as well as a lower number of connected components. For $r = 1, 3, 4, 6$ and 8, as well as varying g and higher N , see S2 Fig, S2 Appendix, S3 Appendix, S3 Fig and S4 Fig.

<https://doi.org/10.1371/journal.pcsy.0000051.g004>

share of the population, such as shown in Fig 3 for $r = 3$ (upper right panel). One conspicuous difference, however, from the results of varying r , is that the increases in these measures with N each show a clear ‘plateau’ value of N after which they remain constant. This is due to the model still being constrained by a constant value of r . Though the space becomes increasingly crowded, agents are still limited to connect to the agents in their covered area $2\pi r$, limiting both the possible closed triangles and the shortest possible path between distant agents that population density can achieve. A similar bounding effect of r is visible in average degree: though average degree increases with population size, the values stay far from their maximum $N-1$. In general, as population density tends towards the point where each coordinate is occupied by an agent, $N/g^2 = 1$, agents tend toward a uniform state characterized by a number of connections equal to the number of coordinates in their ranged area, $2\pi r$. The possible degree, complete triangles, and shortest paths are set in this situation by the size of this area, which is defined by r . For discussion of results at other constant values of r and of varying g , see S2 Appendix, S2 Fig, S3 Appendix, and S4 Fig.

3.3. Information diffusion on range model networks replicates known results.

In addition to tracking network properties outputs, our simulations included four commonly modelled processes of information diffusion on the networks. We simulated a simple contagion process, where ‘susceptible’ agents can be infected by connected ‘infected’ agents with varying probability $P(\text{infect})$; a complex contagion, where $P(\text{infect})$ increases with the number of connected infected agents; a basic cultural evolution model, where two traits each have their own probability of transmission; and a model of the more specific ‘potion task’ process. In a potion task, based on an experiment by Derex and Boyd [4], individuals start with an item inventory, can combine some items into progressively more complex items, and can share known combinations. In the first three processes, we track the timesteps until the state has spread to all agents. In simple and complex contagion, this is reached when the entire population reaches the “infected” state. In the cultural evolution case, this means that one of the traits stochastically comes to dominate and reaches ‘fixation’. In the potion task, we instead track whether a ‘crossover event’ happened after 100 timesteps. A crossover event is a term specific to the potion task, in which there are two ‘trajectories’ of increasingly complex combinations of items, and the most complex item of each trajectory combines into the final ‘crossover’ item. More details on implementation as well as figures are found in S4 Appendix, S5 Fig and S6 Fig. Here, we briefly summarize the expected and observed results.

The expectations from prior research [6,9,44,47] are as follows. As discussed above, high clustering and average shortest path length describe networks that have a delaying effect on transmission. This is true specifically for transmission processes that are based on individual-to-individual transmission probabilities: in this case, the simple contagion, cultural evolution, and potion task processes. Previous research also shows that in the potion task, network properties that delay transmission lead to higher rates of successful crossover events because the population is less likely to get stuck in a single trajectory of possible combinations [3–5]. Finally, in the case of complex contagion, higher clustering is known to speed up rather than delay diffusion, since there is a higher chance of individuals being exposed to multiple same-state neighbors [1]. Accordingly, in the range model and especially at lower r , where we observe higher average shortest path length and higher clustering than in the non-spatial model, we expect slower time to full diffusion in the simple contagion process, and slower trait fixation in cultural evolution. Furthermore, we expect higher crossover event rates and faster complex contagion.

Our simulations replicate these known effects. In simple contagion, the proportion of infected agents increases slightly faster in the null model at each parameter setting tested, from $r = 1$ and $P(\text{connect} = 0.1)$ to $r = 9$ and $P(\text{connect}) = 0.9$ ($N = 10, g = 10$), showing higher differences when range is low. Similarly, traits reach fixation faster at most settings in the cultural evolution model, especially so at higher values of r and $P(\text{connect})$, where we observe more connected (higher average degree) networks. The network structure properties created by range constraints have an especially large effect on complex contagion, where at lower values of r ($r = 1, 2, 3, P(\text{connect}) = 0.1, 0.2, 0.3, N = 10, g = 10$) the proportion of infected individuals increases with more than double the rate observed in the null model. Finally, in the potion task, the expected result is achieved at $r = 1, 2$ ($P(\text{connect}) = 0.1, 0.2; N = 10, g = 10$). On average, across 100 rounds of 100 timesteps, the range model population achieves crossover events in 72 rounds at $r = 1$, versus 32 in the null model ($P(\text{connect}) = 0.1$). The range model maintains a slight advantage (74 versus 70) at $r = 2$. Interestingly, however, at higher settings, the null model performs better (by 9 events on average). A possible explanation could be found in the higher number of connected components observed in the null model. For a more

detailed discussion of network forces that can influence the motion task and how they relate to our simulations, see the S4 Appendix. Overall, our diffusion tests illustrate and quantify the possible consequences of this paper's main results: that spatial constraints have a major influence on our predictions of network structure between individuals. It follows that spatial constraints impact our predictions of the collective processes that take place on these networks.

3.4. Results summary

To summarize the simulation results, we found three major network formation mechanisms introduced by a coordinate space, random movement, and ranged interaction. First, for any constant population size, the ratio of r to g determines how densely connected graphs are, from disconnected agents at $r = 0$ to fully connected networks when $r > g$ (not precisely at $r = g$ because the circular Euclidean ranges do not overlap exactly with the square grid). Second, independently from range, increasing the population density N/g^2 also increases graph density, as agents 'crowd' the coordinate space, making connections more likely. The impact of increasing population density on graph structures is still constrained by r , each node relying on movement for connection when population density is low, but reaching the maximum degree and clustering possible under the current value of r when the population density reaches 1. Range (relative to coordinate space size g) therefore sets the slope of the increase of average degree with population density, as well as 'plateau' maximum values to the increase in clustering, decrease in average shortest path length, and decrease in number of connected components. Finally, range model graphs are more clustered and have lower average shortest path length overall due to the higher probability of connecting to proximate agents, especially at lower $r:g$. In other words, in this model of spatially constrained randomly moving agents, when range constraints are very strict, much of the work of connections is done by movement, which is in turn restricted by the population density. This situation generates highly clustered graphs. Conversely, as range constraints are loosened, movement and position starts to matter less, until they become irrelevant when $r > g$. Finally, we confirm that these differences in network structures impact the behavior of diffusion processes in ways predicted by prior literature.

4. Discussion

In this paper, we report simulations demonstrating that including spatial constraints on agent interactions introduces significant differences in network architectures, and by extension, in information flow. In general but especially when range is low compared to environment size g , since spatial constraints 'assort' agents by physical proximity, networks are more clustered, have higher average shortest path length, a lower number of connected components, and a higher small-world index than dynamic random graphs. Two main parameters drive average network structures: communication range r , relative to g , and population density N/g^2 . As either increases while the other remains constant, graphs become more densely connected. The influence of population density on graph density is bounded by r , limiting the possible connections agents can make. As population density increases, movement becomes increasingly impossible as every agent occupies one of the $g \times g$ coordinates when $N = g^2$. As a result, positions become fixed and node properties become global, set by the value of r . A specific mechanism that causes higher clustering and average shortest path lengths in range model networks is that any agents j connecting to an agent i need to be within the area covered by i 's range, significantly increasing the probability that agents j connect to each other as well.

We also show that range model networks create more small-world like networks than a non-spatial model, and that diffusion processes are impacted indirectly by spatial constraints as a result of their impact on network structure.

These results on clustering and small-world index bear repeating. When human networks are compared to other systems such as technological and biological networks, high clustering consistently shows up as a distinguishing characteristic [33,44,48,49]. When this high clustering is combined with relatively low average shortest path length, networks become well-described as small world networks, a type of network that was designed to exhibit characteristics of human networks [44]. Our simulations show that such network properties can be the result of simply situating communication in space and assuming random movement. Similar results were found for static random networks by Wong and colleagues, who found high clustering and low average shortest path length as a result of introducing ranged connection in an unbounded space [49]. We reproduce these findings for a dynamic model, the full range of N , g , and r , and in bounded spaces. The fact that 'human-like' networks can be consistently produced from random movement and spatial constraints alone raises questions about the relative contribution of spatial and social mechanisms to network structures. Are these human properties to be explained by social preferences specific to intelligent social species, or can they also be explained by physical properties that are common to all moving communicating systems? An interesting direction for future models and experiments would be to study the interaction between spatial constraints and the preferences, strategies and biases of social connecting hypothesized by existing literature [10–19]. Our model provides a tool to track interaction partners that are possible under spatial constraints, while leaving open the possibility of adding preferential connection rules for agents to select from this subset while in range.

One obvious but central result of our simulations is that when r exceeds grid size g , fully connected networks are guaranteed. In other words, $r > g$ is the condition that needs to obtain before each individual has access to each other individual. By extension, this is the condition that needs to obtain before individual choices, strategies, and biases about who to connect to and communicate with can fully account for network formation. Our simulations quantify what happens when this condition does not obtain (when $0 < r < g$), and when therefore spatial constraints play a role in network formation.

One mechanism that starts to play a role in network formation when $r > g$ is mobility. In their paper reporting a similar model, Vining and colleagues discuss a distinction between solid and liquid brains [35]. Solid brains, such as human brains and computer chips, have elements and links in more or less fixed positions, whereas liquid brains, such as swarms and slime moulds, consist of mobile elements that form transient links [50]. Vining and colleagues note that in liquid brains, mobility can play the role that physical links can play otherwise: connecting nodes, creating a pathway enabling information sharing. This is what we see in our simulations when $r > g$: because agents are situated in an environment and communication is range-constrained, moving through that environment becomes a mechanism for network formation. As $r:g$ decreases, mobility becomes the dominant mechanism for connection; as $r:g$ increases, links take over. This, too, is an interesting dynamic in light of the discussion of social versus spatial contributions to network structure: we expect preferences of selective connection to dominate when $r:g$ is close to 1, while mobility and environmental constraints do so when $r:g$ is low. Additionally, as population density increases, and the stochastic element of our model (random movement) slowly disappears, agent network properties becomes increasingly global and determined by r as the coordinate space becomes saturated and mobility becomes impossible. One interesting consequence is that, as the mobility mechanism disappears, models of networks on fixed lattices may therefore become more applicable in systems under 'crowded' circumstances. Small-world networks, for example, are partly

generated by a parameter k which connects each agent to the k nearest neighbors on a lattice, and as a consequence setting a global node degree k [44]. In the fully ‘crowded’ settings of our model where $N/g^2 = 1$, r functions the same way, setting a global node degree equal to the number of integer coordinates that fall within an agent’s range, $2\pi r$.

Real individuals will of course show more intelligent mobility patterns than random movement. Moreover, random movement can be implemented in ways different from our model. A more standard implementation of movement direction in agent-based models is for agents to select from a uniform distribution of angles rather than directly from integer coordinate ‘tiles.’ In a recent paper, Chimento and Farine simulated this implementation of random movement as well as movement patterns where the distribution of angles was more concentrated towards specific directions, and where agents move towards resources in the environment [34]. Alternatively, using data from cell phone towers, researchers have found that human displacements over time are approximated by so-called Lévy flight processes, where agents select step sizes from a power-law distribution of distances. Most of us move small to no distances most of the time, and greater distances some of the time; in addition, a small number of people travels much greater distances [51,52]. One direction for future work is to combine our results of varying range and population size with these more realistic mobility patterns, and to test the fit of different mobility patterns to observational data of human communication and other interaction networks, employing our model to see the role of spatial constraints to interindividual interactions in the real world.

Apart from mobility, as discussed, we found a role for population size and density in the formation of networks. The role of population size in transmission processes has been discussed in literature on models in cultural evolution. Models have demonstrated that greater population size, under the right demographic and network connectivity circumstances, increases a population’s ability to create and maintain complex skills [3,53–55]. Our simulations show a different role for population size: increasing N in a bounded space increases population density, increasing the probability for randomly moving agents to encounter each other, creating more dense networks for interaction. Under the spatial constraints of a bounded environment and limited-range communication, population size influences not just transmission networks, where links are the information actually transmitted, but the communication network infrastructure that makes transmission possible, where links are the possible pathways for information transmission.

One limitation of the present work is that though we quantify the impact of a bounded environment, the space itself is empty and unobstructed. The structure of real environments might significantly impact the possibilities of communication, introducing more complexity as well as realism into the spatial computation of network structure. A second limitation is that we consider only single-layer networks with global values for communication range, while real communicating systems may use different and overlapping communication media and technologies with different effective ranges. A third limitation is that we compare the ranged model to only one type of non-spatial model. Comparison to (dynamic versions of) other ‘standard’ non-spatial network generation algorithms such as small-world and preferential attachment graphs [44,56,57] would paint a broader picture of the impact of including spatial constraints in network generation algorithms. All three of these limitations would be fruitful directions for future work.

Leaving the role of spatial constraints out of the picture (for example, by over-relying on digital communication data, social surveys, experimental settings where participants are all in the same space, or traditional network generation algorithms) could lead one to suggest that the mechanisms driving human network formation are primarily in psychology and behavior. However, including them in a model shows that, compared to a non-spatial model, these

constraints alone can have a major impact on our predictions of network structure, and generate human-like networks. In any real system of individuals, of course, spatial and social contributions to network structure will not be mutually exclusive or even independent, and studying the relative contribution and interaction of both is imperative. One advantage, however, of physical properties such as location and communication range as a partial explanatory mechanism of real networks is that they are much more straightforward to interpret, test and implement than hypotheses about drivers of human psychology and behavior. The model reported in this paper provides a tool to understand interaction networks as the product of a process of collective computation which does not just include cognitive heuristics by isolated individuals, but also their embeddedness in an environment.

Supporting information

S1 Appendix. Full results of varying r .
(PDF)

S2 Appendix. Full results of varying N .
(PDF)

S3 Appendix. Varying g .
(PDF)

S4 Appendix. Transmission processes.
(PDF)

S1 Fig. Network properties of range model (blue) and null model (red) networks for varying r between 1 and 10 for $g = 10$ and $N = 20, 40, 60, 80$.
(PDF)

S2 Fig. Network properties of range model (blue) and null model (red) networks for varying N between 1 and 49 for $g = 7$ and $r = 1, 2, 3, 4, 6, 8$.
(PDF)

S3 Fig. Network properties of range model (blue) and null model (red) networks for varying N between 1 and 100 (x-axes), $g = 10$, $r = 2$.
(PDF)

S4 Fig. Network properties of range model networks for varying g between 1 and 50 (x-axes), $r = 2$, $N = 10$.
(PDF)

S5 Fig. Trait frequencies over time (SI diffusion, top; complex contagion, second from top; biased transmission, third from top) for $N = 10$, $g = 10$; and potion task crossover events out of 100 timesteps for $N = 80$, as range varies between 0 and 10; left panels range model, right panels null model.
(PDF)

S6 Fig. Trait frequencies over time (SI diffusion, top; complex contagion, second from top; biased transmission, third from top) for $r = 2$, $g = 10$; and potion task crossover events out of 100 timesteps, N varying between 1 and 24; left panels range model, right panels null model.
(PDF)

Author contributions

Conceptualization: Niek Kerssies, Jose Segovia-Martin, James Winters.

Formal analysis: Niek Kerssies.

Investigation: Niek Kerssies.

Methodology: Niek Kerssies, Jose Segovia-Martin, James Winters.

Supervision: Jose Segovia-Martin, James Winters.

Visualization: Niek Kerssies.

Writing – original draft: Niek Kerssies.

Writing – review & editing: Niek Kerssies, Jose Segovia-Martin, James Winters.

References

1. Centola D. The spread of behavior in an online social network experiment. *Science*. 2010;329(5996):1194–7. <https://doi.org/10.1126/science.1185231> PMID: 20813952
2. Centola D, Baronchelli A. The spontaneous emergence of conventions: an experimental study of cultural evolution. *Proc Natl Acad Sci U S A*. 2015;112(7):1989–94. <https://doi.org/10.1073/pnas.1418838112> PMID: 25646462
3. Moser C, Smaldino PE. Innovation-facilitating networks create inequality. *Proc Biol Sci*. 2023;290(2011):20232281. <https://doi.org/10.1098/rspb.2023.2281> PMID: 37989247
4. Derex M, Boyd R. Partial connectivity increases cultural accumulation within groups. *Proc Natl Acad Sci U S A*. 2016;113(11):2982–7. <https://doi.org/10.1073/pnas.1518798113> PMID: 26929364
5. Derex M, Perreault C, Boyd R. Divide and conquer: intermediate levels of population fragmentation maximize cultural accumulation. *Philos Trans R Soc Lond B Biol Sci*. 2018;373(1743):20170062. <https://doi.org/10.1098/rstb.2017.0062> PMID: 29440527
6. Lazer D, Friedman A. The network structure of exploration and exploitation. *Administ Sci Quart*. 2007;52(4):667–94. <https://doi.org/10.2189/asqu.52.4.667>
7. Bavelas A. Communication patterns in task-oriented groups. *J Acoust Soc Am*. 1950;22(6):725–30. <https://doi.org/10.1121/1.1906679>
8. Momennejad I. Collective minds: social network topology shapes collective cognition. *Philos Trans R Soc Lond B Biol Sci*. 2022;377(1843):20200315. <https://doi.org/10.1098/rstb.2020.0315> PMID: 34894735
9. Centola D. The network science of collective intelligence. *Trends Cogn Sci*. 2022;26(11):923–41. <https://doi.org/10.1016/j.tics.2022.08.009> PMID: 36180361
10. Redhead D, Power EA. Social hierarchies and social networks in humans. *Philos Trans R Soc Lond B Biol Sci*. 2022;377(1845):20200440. <https://doi.org/10.1098/rstb.2020.0440> PMID: 35000451
11. Rivera MT, Soderstrom SB, Uzzi B. Dynamics of dyads in social networks: assortative, relational, and proximity mechanisms. *Annu Rev Sociol*. 2010;36(1):91–115. <https://doi.org/10.1146/annurev.soc.34.040507.134743>
12. Conte A, Di Cagno D, Sciubba E. Strategies in social network formation. *Theory Decis*. 2009;67(2):161–93.
13. Almaatouq A, Noriega-Campero A, Alotaibi A, Krafft PM, Moussaid M, Pentland A. Adaptive social networks promote the wisdom of crowds. *Proc Natl Acad Sci U S A*. 2020;117(21):11379–86. <https://doi.org/10.1073/pnas.1917687117> PMID: 32393632
14. Nakayama S, Krasner E, Zino L, Porfiri M. Social information and spontaneous emergence of leaders in human groups. *J R Soc Interface*. 2019;16(151):20180938. <https://doi.org/10.1098/rsif.2018.0938> PMID: 30958196
15. Kendal RL, Boogert NJ, Rendell L, Laland KN, Webster M, Jones PL. Social learning strategies: bridge-building between fields. *Trends Cogn Sci*. 2018;22(7):651–65. <https://doi.org/10.1016/j.tics.2018.04.003> PMID: 29759889
16. Boyd R, Richerson PJ. *Culture and the evolutionary process*. Chicago, IL: University of Chicago Press. 1985.
17. Laland KN. Social Learning Strategies. *Learn Behav*. 2004;32(1):4–14.

18. Canteloup C, Hoppitt W, van de Waal E. Wild primates copy higher-ranked individuals in a social transmission experiment. *Nat Commun.* 2020;11(1):459. <https://doi.org/10.1038/s41467-019-14209-8> PMID: 31974385
19. Kendal R, Hopper LM, Whiten A, Brosnan SF, Lambeth SP, Schapiro SJ, et al. Chimpanzees copy dominant and knowledgeable individuals: implications for cultural diversity. *Evol Hum Behav.* 2015;36(1):65–72. <https://doi.org/10.1016/j.evolhumbehav.2014.09.002> PMID: 27053916
20. Smith JE, Natterson-Horowitz B, Alfaro ME. The nature of privilege: intergenerational wealth in animal societies. *Behavioral Ecology.* 2022;33(1):1–6. <https://doi.org/10.1093/beheco/arab137>
21. Borgerhoff Mulder M, Bowles S, Hertz T, Bell A, Beise J, Clark G, et al. Intergenerational wealth transmission and the dynamics of inequality in small-scale societies. *Science.* 2009;326(5953):682–8. <https://doi.org/10.1126/science.1178336> PMID: 19900925
22. Cantor M, Whitehead H. The interplay between social networks and culture: theoretically and among whales and dolphins. *Philos Trans R Soc Lond B Biol Sci.* 2013;368(1618):20120340. <https://doi.org/10.1098/rstb.2012.0340> PMID: 23569288
23. Ilany A, Holekamp KE, Akçay E. Rank-dependent social inheritance determines social network structure in spotted hyenas. *Science.* 2021;373(6552):348–52. <https://doi.org/10.1126/science.abc1966> PMID: 34437155
24. Bokányi E, Heemskerk EM, Takes FW. The anatomy of a population-scale social network. *Sci Rep.* 2023;13(1):9209. <https://doi.org/10.1038/s41598-023-36324-9> PMID: 37280385
25. Piketty T. About capital in the twenty-first century. *Am Econ Rev.* 2015;105(5):48–53.
26. Gemar A. Parental status connection and social network variety in adulthood. *Societies.* 2024;14(2):26. <https://doi.org/10.3390/soc14020026>
27. Cowgill B, Wolfers J, Zitzewitz E. Using prediction markets to track information flows: Evidence from Google. In: Das S, Ostrovsky M, Pennock D, Szymanski B, editors. *Auctions, market mechanisms and their applications.* Berlin, Heidelberg: Springer; 2009. p. 3.
28. Stopczynski A, Pentland A “Sandy”, Lehmann S. How physical proximity shapes complex social networks. *Sci Rep.* 2018;8(1):17722. <https://doi.org/10.1038/s41598-018-36116-6> PMID: 30531809
29. Tóth G, Wachs J, Di Clemente R, Jakobi Á, Ságvári B, Kertész J, et al. Inequality is rising where social network segregation interacts with urban topology. *Nat Commun.* 2021;12(1):1143. <https://doi.org/10.1038/s41467-021-21465-0> PMID: 33602929
30. Acerbi A. *Cultural evolution in the digital age.* Cambridge, MA: MIT Press; 2020.
31. Backstrom L, Boldi P, Rosa M, Ugander J, Vigna S. The anatomy of the Facebook social graph. In: *Proceedings of the 21st International Conference on World Wide Web.* 2011. p. 831–40.
32. Bokányi E, Novák M, Jakobi Á, Lengyel B. Urban hierarchy and spatial diffusion over the innovation life cycle. *R Soc Open Sci.* 2022;9(5):211038. <https://doi.org/10.1098/rsos.211038> PMID: 35592759
33. Onnela JP, Saramáki J, Hyvönen J, Szabó G, Lazer D, Kaski K. Structure and tie strengths in mobile communication networks. *Proc Natl Acad Sci U S A.* 2007;104:7332–6.
34. Chimento M, Farine DR. The contribution of movement to social network structure and spreading dynamics under simple and complex transmission. *Philos Trans R Soc Lond B Biol Sci.* 2024;379(1912):20220524. <https://doi.org/10.1098/rstb.2022.0524> PMID: 39230450
35. Vining WF, Esponda F, Moses ME, Forrest S. How does mobility help distributed systems compute? *Philos Trans R Soc Lond B Biol Sci.* 2019;374(1774):20180375. <https://doi.org/10.1098/rstb.2018.0375> PMID: 31006367
36. Davis GH, Crofoot MC, Farine DR. Using optimal foraging theory to infer how groups make collective decisions. *Trends Ecol Evol.* 2022;37(11):942–52. <https://doi.org/10.1016/j.tree.2022.06.010> PMID: 35842325
37. Zollman KJS. The communication structure of epistemic communities. *Philos of Sci.* 2007;74(5):574–87. <https://doi.org/10.1086/525605>
38. Winters J. Escaping optimization traps: the role of cultural adaptation and cultural exaptation in facilitating open-ended cumulative dynamics. *Palgrave Commun.* 2019;5(1). <https://doi.org/10.1057/s41599-019-0361-3>
39. Axelrod R. The dissemination of culture. *J Conflict Resolut.* 1997;41(2):203–26. <https://doi.org/10.1177/0022002797041002001>
40. Langbauer WR. Elephant communication. *Zoo Biol.* 2000;19(5):425–45. [https://doi.org/10.1002/1098-2361\(2000\)19:5<425::aid-zoo11>3.0.co;2-a](https://doi.org/10.1002/1098-2361(2000)19:5<425::aid-zoo11>3.0.co;2-a)
41. Kota M, Olzer R. Insect communication. In: Vonk J, Shackelford TK, editors. *Encyclopedia of animal cognition and behavior.* 2022. p. 3465–71.

42. Brila I, Lavrinienko A, Tukalenko E, Kallio ER, Mappes T, Watts PC. Idiosyncratic effects of coinfection on the association between systemic pathogens and the gut microbiota of a wild rodent, the bank vole *Myodes glareolus*. *J Anim Ecol*. 2023;92(4):826–37. <https://doi.org/10.1111/1365-2656.13869> PMID: 36504351
43. Mateo D, Horsevad N, Hassani V, Chamanbaz M, Bouffanais R. Optimal network topology for responsive collective behavior. *Sci Adv*. 2019;5(4):eaau0999. <https://doi.org/10.1126/sciadv.aau0999> PMID: 30949570
44. Watts DJ, Strogatz SH. Collective dynamics of ‘small-world’ networks. *Nature*. 1998;393(6684):440–2.
45. Humphries MD, Gurney K. Network “small-world-ness”: a quantitative method for determining canonical network equivalence. *PLoS One*. 2008;3(4):e0002051. <https://doi.org/10.1371/journal.pone.0002051> PMID: 18446219
46. Erdős P, Rényi A. On random graphs. *Publicationes Mathematicae Debrecen*. 1959;6:290–7.
47. Barabási A-L, Albert R, Jeong H. Scale-free characteristics of random networks: the topology of the world-wide web. *Phys A: Statist Mech Appl*. 2000;281(1–4):69–77. [https://doi.org/10.1016/s0378-4371\(00\)00018-2](https://doi.org/10.1016/s0378-4371(00)00018-2)
48. Ugander J, Karrer B, Backstrom L, Marlow CA. The anatomy of the Facebook social graph. *arXiv*. 2011.
49. Wong LH, Pattison P, Robins G. A spatial model for social networks. *arXiv preprint*. 2005. <https://arxiv.org/abs/physics/0505128>
50. Solé R, Moses M, Forrest S. Liquid brains, solid brains. *Philos Trans R Soc Lond B Biol Sci*. 2019;374(1774):20190040. <https://doi.org/10.1098/rstb.2019.0040> PMID: 31006374
51. González MC, Hidalgo CA, Barabási A-L. Understanding individual human mobility patterns. *Nature*. 2008;453(7196):779–82. <https://doi.org/10.1038/nature06958> PMID: 18528393
52. Almaatouq A, Prieto-Castrillo F, Pentland A. Mobile communication signatures of unemployment. In: Aiello LM, McFarland D, editors. *Computational social science: discovery and prediction*. 2016. p. 413–28.
53. Baldini R. Revisiting the effect of population size on cumulative cultural evolution. *J Cogn Cult*. 2015;15(3–4):320–36. <https://doi.org/10.1163/15685373-12342153>
54. Deffner D, Kandler A, Fogarty L. Effective population size for culturally evolving traits. *bioRxiv*. 2021.
55. Henrich J. Demography and cultural evolution: how adaptive cultural processes can produce maladaptive losses—the tasmanian case. *Am Antiq*. 2004;69(2):197–214. <https://doi.org/10.2307/4128416>
56. Watts DJ. Networks, dynamics, and the small-world phenomenon. *Am J Sociol*. 1999;105(2):493–527. <https://doi.org/10.1086/210318>
57. Barabási A-L, Albert R, Jeong H. Scale-free characteristics of random networks: the topology of the world-wide web. *Phys A: Statist Mech Appl*. 2000;281(1–4):69–77. [https://doi.org/10.1016/s0378-4371\(00\)00018-2](https://doi.org/10.1016/s0378-4371(00)00018-2)